Acetylation regulates tropomyosin function in the fission yeast *Schizosaccharomyces pombe*

Kalomoira Skoumpla[1,*], Arthur T. Coulton[2,*], William Lehman[3], Michael A. Geeves[2] and Daniel P. Mulvihill[1,‡]

[1]Cell and Developmental Biology Group and [2]Protein Science Group, Department of Biosciences, University of Kent at Canterbury, Canterbury, CT2 7NJ, UK
[3]Department of Physiology and Biophysics, Boston University School of Medicine, Boston, MA 02118, USA
*These authors contributed equally to this work
‡Author for correspondence (e-mail: d.p.mulvihill@kent.ac.uk)

Accepted 5 March 2007
Journal of Cell Science 120, 1635-1645 Published by The Company of Biologists 2007
doi:10.1242/jcs.001115

Summary

Tropomyosin is an evolutionarily conserved α-helical coiled-coil protein that promotes and maintains actin filaments. In yeast, Tropomyosin-stabilised filaments are used by molecular motors to transport cargoes or to generate motile forces by altering the dynamics of filament growth and shrinkage. The *Schizosaccharomyces pombe* tropomyosin Cdc8 localises to the cytokinetic actomyosin ring during mitosis and is absolutely required for its formation and function. We show that Cdc8 associates with actin filaments throughout the cell cycle and is subjected to post-translational modification that does not vary with cell cycle progression. At any given point in the cell cycle 80% of Cdc8 molecules are acetylated, which significantly enhances their affinity for actin. Reconstructions of electron microscopic images of actin-Cdc8 filaments establish that the majority of Cdc8 strands sit in the 'closed' position on actin filaments, suggesting a role in the regulation of myosin binding. We show that Cdc8 regulates the equilibrium binding of myosin to actin without affecting the rate of myosin binding. Unacetylated Cdc8 isoforms bind actin, but have a reduced ability to regulate myosin binding to actin. We conclude that although acetylation of Cdc8 is not essential, it provides a regulatory mechanism for modulating actin filament integrity and myosin function.

Supplementary material available online at
http://jcs.biologists.org/cgi/content/full/120/9/1635/DC1

Key words: Acetylation, Actin, Tropomyosin, Cdc8, *Schizosaccharomyces pombe*, Fission yeast

Introduction

Tropomyosin (Tm) is an evolutionarily conserved linear α-helical coiled-coil actin binding protein that is required for the stabilisation and maintenance of actin filaments within eukaryotic cells (Perry, 2001). Tm polymerises to form strands that associate with actin filaments and provide structural stability as well as providing a strategy for modulating actin filament formation and function in muscle cells. These Tm-stabilised actin filaments facilitate the execution of a plethora of actin-cytoskeleton-dependent cellular processes including cytokinesis, organelle transport, endocytosis and muscle contraction. The best characterised role of Tm is in the regulation of muscle contraction, where the protein modulates the association between actin and myosin; however, non-muscle Tms play an important role in stabilising and modulating the function of the F-actin component of cellular microfilaments (Gunning et al., 2005). Immunochemical staining localises Tm within continuous dynamic microfilaments in stress fibres, microfilament meshworks, polygonal networks and contractile rings. Acetylation of the N-terminal methionine of mammalian Tm is required for these proteins to associate with actin (Monteiro et al., 1994; Urbancikova and Hitchcock-DeGregori, 1994). Structural studies suggest that this amino acetylation brings about a conformational change, stabilising the amino coiled-coil structure thus promoting polymerisation through head-to-tail interactions (Brown et al., 2001; Palm et al., 2003). By contrast, fibroblast Tm variants do not require N-terminal acetylation because these splice variants have an N-terminal extension that may stabilise the protein amino coiled-coil structure and thus promote filament formation (Pittenger and Helfman, 1992).

Simple unicellular eukaryotes such as yeast have provided a unique model system to study the function of Tm. The genome of the budding yeast *Saccharomyces cerevisiae* contains two tropomyosin genes *TPM1* and *TPM2* encoding proteins with non-overlapping functions (Drees et al., 1995; Liu and Bretscher, 1989). These are shorter than metazoan tropomyosins, which associate with either six or seven actin monomers, in contrast to the five and four actin monomers predicted for Tpm1 and Tpm2, respectively. Although deleting the *TPM2* gene from the genome has no obvious consequence, *TPM1* is an essential gene required for the function of the type V myosin, Myo2p (Drees et al., 1995; Liu and Bretscher, 1992; Schott et al., 1999). Consistent with studies from other organisms, budding yeast Tpm1 has also been shown to be acetylated at its N-terminus (Polevoda et al., 2003; Singer and Shaw, 2003).

By contrast, the genome of the fission yeast *Schizosaccharomyces pombe* contains a single tropomyosin gene, *cdc8*$^{+}$, which encodes a protein of 161 amino acids (Balasubramanian et al., 1992). The Cdc8 protein is required

for the formation and maintenance of actin filaments during both mitotic and meiotic lifecycles (Balasubramanian et al., 1992; Kurahashi et al., 2002; Pelham and Chang, 2001). It localises to the cytokinetic actomyosin ring (CAR) during mitosis, where it plays an essential role during cytokinesis (Balasubramanian et al., 1992). Strains lacking functional Cdc8 fail to septate yet continue to undergo nuclear division, resulting in the accumulation of long multinucleate aseptate cells.

Here we report a comprehensive cross-disciplinary study encompassing the fields of cell and molecular biology, biochemistry and structural biology to examine the properties of the fission yeast tropomyosin, Cdc8. We localised Cdc8 at both the cellular and structural level. We show that it associates with actin filaments with a specific pattern of localisation through the entire cell cycle. Biochemical analyses indicate that Cdc8 levels remain constant throughout the cell cycle, and 80% of the protein is consistently acetylated. We go on to show that this acetylation alters the ability of the protein to associate with actin and regulate myosin.

Results

Characterisation of anti-Cdc8 antisera

Antibodies were generated against full-length heterologously expressed untagged Cdc8 protein. Western blot analysis confirmed the specificity of the anti-Cdc8 antisera (Fig. 1A). A single band was detected on 10% SDS-PAGE gels corresponding to ~27 kDa in extracts from wild-type cells (Fig. 1A, lane 1). Reduced mobility of Cdc8 is likely to be a consequence of its coiled-coil nature. The intensity of this band was markedly increased in extracts prepared from cells in which Cdc8 was additionally expressed from the multicopy plasmid pREP41*cdc8*$^{+}$ (Fig. 1A, lane 2). An additional band of equal intensity to the endogenous protein migrated at ~52 kDa in extracts prepared from DPM703 cells expressing N-terminally tagged GFP-Cdc8 from an integrant copy of the *gfp-cdc8* gene under the control of the *nmt41* promoter (Fig. 1A, lane 3). An identical GFP-Cdc8 band pattern was revealed when the membrane was probed with anti-GFP antibody (Fig. 1B, lane 3). These results demonstrate the anti-Cdc8 sera specifically recognises the Cdc8 protein and also that protein expression is equivalent from the integrated INT*nmt41* vector and the endogenous *cdc8*$^{+}$ promoter.

Cdc8 protein levels do not change throughout the cell division cycle

Cdc8 has been reported to localise to the CAR during mitosis (Balasubramanian et al., 1992), we therefore explored whether Cdc8 levels fluctuate during the cell cycle. *cdc25-22 myo2-gc* cells were synchronised and allowed to grow for two full cell division cycles (Fig. 1D), and samples taken for fluorescence microscopy and biochemical analysis. Western blot analysis of the extracts using the anti-Cdc8 sera revealed that the protein migrated as a doublet, with ~80% of the protein always present in the faster migrating band. Fluctuations in Cdc8 levels did not accompany cell cycle progression through the cell division cycle (Fig. 1E). Measurements comparing the intensity of the Cdc8 doublets to the α-tubulin (Fig. 1F) revealed that the ratio of Cdc8 to α-tubulin levels did not fluctuate detectably.

Cdc8 localises to actin filaments during interphase

Immunofluorescence revealed that Cdc8 localised to filaments, which extended throughout the length of the cell during interphase. The filaments were seen in cells throughout G2 (Fig. 2Ai-iii), until the onset of mitosis (Fig. 2Aiv), when the Cdc8 filaments extended around the cell equator (Fig. 2Aiv-vii). Simultaneous staining with anti-Cdc8 and TAT1 antibodies revealed Cdc8 filaments incorporated into the nascent CAR in cells possessing a short pro-metaphase spindle (Fig. 2B). Upon completion of mitosis, Cdc8 filaments extended from the edges of the CAR (Fig. 2Avii) into the subsequent daughter cells. Cdc8 filaments can clearly be seen

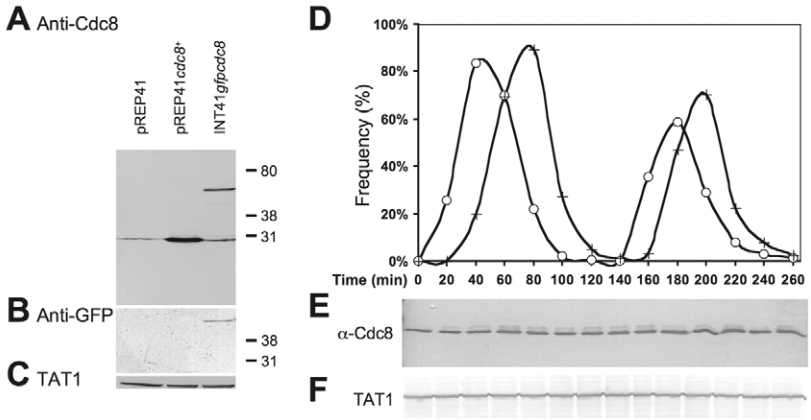

Fig. 1. Cdc8 protein levels do not fluctuate during the cell division cycle. (A) A novel anti-Cdc8 antibody was characterised by western blot of protein extracts from wild-type strains containing either the multicopy plasmid pREP41 (empty vector) or pREP41*cdc8*, or from a wild-type strain in which the plasmid pINT41*gfp-cdc8* had been integrated at the *leu1*$^{+}$ locus. All cells were grown in de-repressed conditions (– thiamine). An extract of wild-type cells containing the empty vector, pREP41, shows a Cdc8 band that migrates at 27 kDa. The intensity of the band increased in wild-type cells in which *cdc8*$^{+}$ was additionally expressed from a plasmid under the control of the nmt41 promoter (pREP41*cdc8*$^{+}$). Extracts from cells expressing chromosome integrated *gfp-cdc8* showed an additional GFP-tagged Cdc8 at ~54kDa, the intensity of which was comparable to the endogenous Cdc8 band. The same GFP-Cdc8 band was seen when the membrane was probed with anti-GFP antibody (B). (C) The same membrane probed with TAT1 to demonstrate equal loading of protein. A population of DPM126 cells were synchronised using transient block and release of the *cdc25-22* allele. Two cell cycles were followed and samples were taken every 20 minutes for western blot analysis and for scoring the appearance of actin rings and septation index at each time point. Positions of molecular mass markers (in kDa) are indicated. (D) The proportion of cells possessing cytokinetic actomyosin rings (O) or a septum (+) at each time point over the two cell cycles. A western blot of whole cell extracts from each time point was probed with both Cdc8 anti-sera (E) and TAT1 antibody (F). Cdc8 migrates as a constant doublet throughout the cell cycle. Quantification of the ratio of TAT1 to Cdc8 doublet signals were analysed from three independent experiments and revealed no fluctuation in Cdc8 levels as cells progress through the cell cycle.

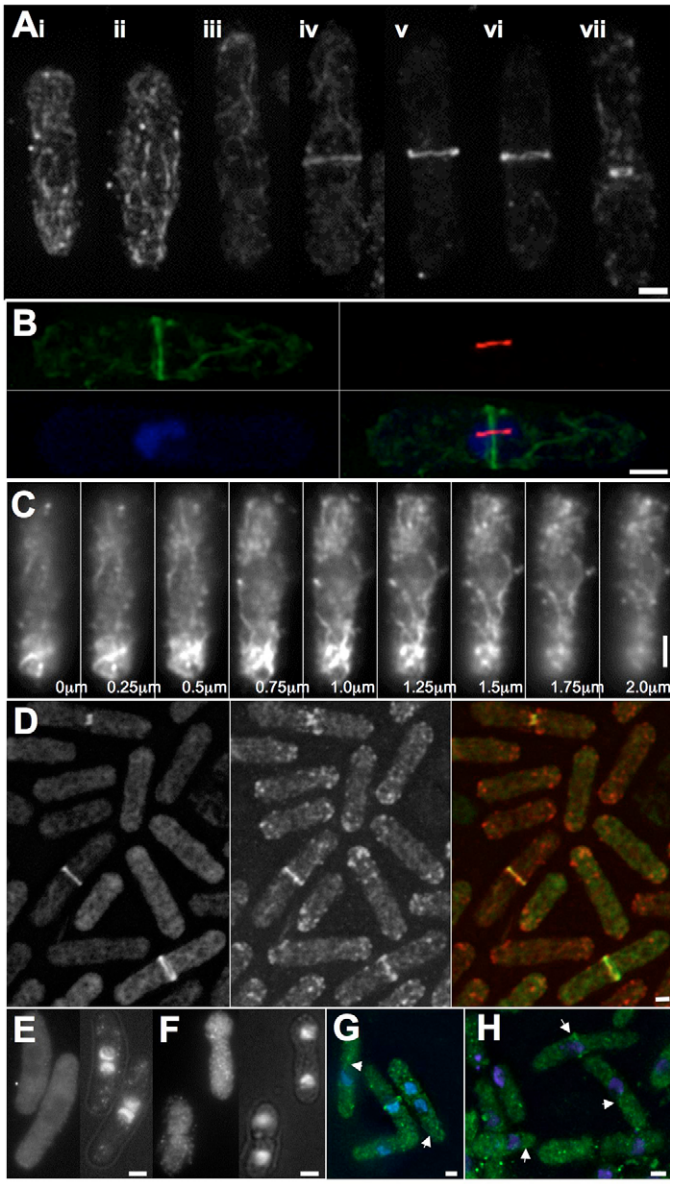

Fig. 2. Cdc8 localises to actin filaments throughout the cell division cycle. (A) Cdc8 immunofluorescence staining of the wild-type strain DPM219 using Cdc8 antiserum. Panels are numbered (i-vii) to show successive cell cycle stages. During G2 (i, ii and iii) Cdc8 localised to filaments that extend to the full length of the cell. Upon entry into mitosis (iv) Cdc8 filaments extend around the cell equator as Cdc8 filaments are incorporated into the CAR, with signal intensity increasing throughout mitosis (v and vi). During contraction, Cdc8 filaments extend out of the CAR into the cytoplasm (vii) to be incorporated into filament structures in the two daughter cells. (B) Co-staining of Cdc8 (green), microtubules (red) and nuclear material (blue) with Cdc8 antisera, TAT1 antibody and DAPI, respectively, revealed that Cdc8 filaments incorporated into a medial ring structure prior to metaphase. (C) A *z*-series through a wild-type cell subjected to Cdc8 immunofluorescence staining. 0.25-μm serial sections extend from the bottom (0 μm) to the top (2.0 μm) of the cell. Filaments can be seen to extend to the full length of the cell. (D) Simultaneous staining with Cdc8 serum (left panel, green in right panel) and Rhodamine-phalloidin (middle panel, red in right panel) demonstrate that Cdc8 colocalises with actin. (E,F) Left panels show Cdc8 localisation and right panels show DAPI phase images of the same cells. Cdc8 filaments were absent in *cdc3-124* cells incubated at the restrictive temperature (E), and in wild-type cells treated with 10 μM Latrunculin A (F), demonstrating Cdc8 filament integrity in vivo requires F-actin. (G,H) Cdc8 localised (green) to the CAR and interphase filaments (arrows) in cells lacking microtubules. DAPI staining (blue) revealing nuclear positioning and fragmentation defects synonymous with microtubule depolymerisation brought about by either *nda2-km52* cells (G), or treating wild type cells with carbendazim (H). Bars, 2 μm.

in serial section images through individual interphase cells (Fig. 2C).

Co-staining cells with anti-Cdc8 sera and Rhodamine-conjugated phalloidin revealed that Cdc8 not only colocalises with actin at the cytokinetic ring during mitosis as previously described, but also colocalises with actin cables during interphase (Fig. 2D, supplementary material Movie 1). To investigate whether Cdc8 filament integrity is dependent upon actin, Cdc8 localisation was examined in cells lacking functional Cdc3, the fission yeast profilin (Balasubramanian et al., 1994). In contrast to wild-type cells mixed into the sample prior to fixation (not shown), Cdc8 failed to localise in temperature-sensitive *cdc3-124* cells cultured at the restrictive temperature (Fig. 2E). In addition, treating wild-type cells with 20 μM Latrunculin A resulted in the disappearance of Cdc8 filaments (Fig. 2F). By contrast, Cdc8 filaments appeared normal in both the tubulin mutant *nda2-km52* (Umesono et al., 1983) (Fig. 2G) and in carbendazim-treated wild-type cells (Fig. 2H). These data demonstrate for the first time that Cdc8 localises to actin filaments during interphase in *S. pombe*.

Cdc8 was also observed directly in live *gfp-cdc8* cells where GFP-Cdc8 expressed from the integrant *gfp-cdc8* allele was able to complement the growth defects associated with the temperature-sensitive *cdc8-110* allele (data not shown). GFP-Cdc8 associated with the CAR (Fig. 3A), where it colocalised with actin (Fig. 3B). Visualisation of GFP-Cdc8 in live fission yeast cells allowed for the first time the opportunity to visualise the highly dynamic actin filaments in vivo during interphase, and follow their incorporation into the CAR during mitosis (Fig. 3C and supplementary material Movie 2). The rate of CAR constriction in these cells is equivalent to that reported previously, providing further evidence of GFP-Cdc8 functionality (Bezanilla et al., 2000; Kitayama et al., 1997; Mulvihill and Hyams, 2002).

The budding yeast Tpm1 and smooth muscle Tm localise in *S. pombe*

We next examined the ability of budding yeast and mammalian Tm to localise (by expressing GFP fusions) and complement Cdc8 function. Genes expressing GFP fusion proteins of each Tm under the control of the nmt41 promoter were integrated at the *leu1* locus within the genome of wild-type *cdc8*$^{+}$ cells. Only the localisation pattern of budding yeast Tpm1 was indistinguishable from that of Cdc8 (Fig. 3D), colocalising with actin (Fig. 3E) and forming contractile rings (Fig. 3F). However, the budding yeast Tpm2, smooth muscle Tm and skeletal muscle Tm all failed to localise to actin filaments and were only seen to concentrate at the cell equator without

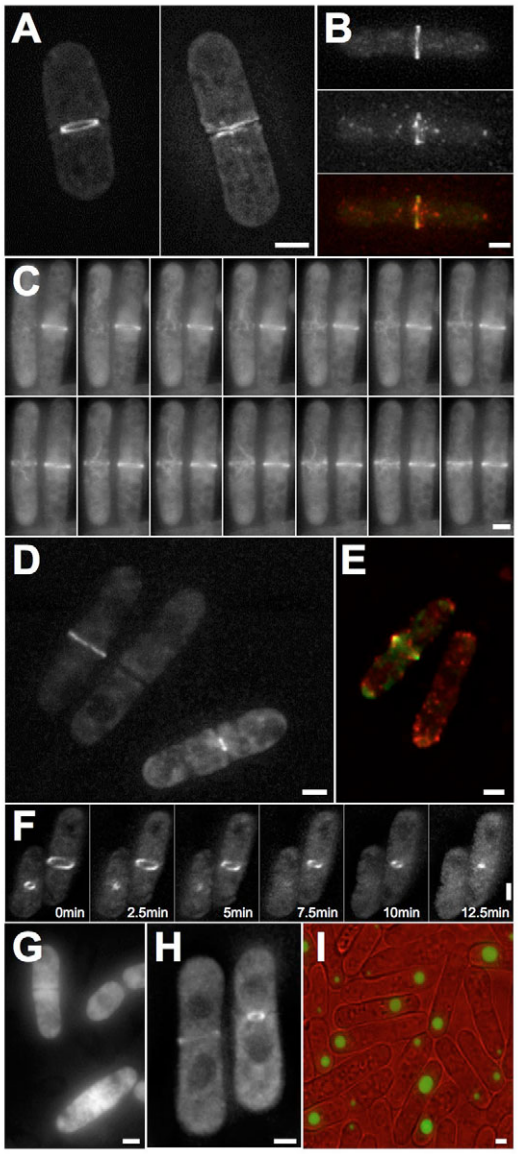

Fig. 3. Localisation of GFP-Tm in *S. pombe*. (A) GFP autofluorescence of live DPM751 cells, show Cdc8 localises to the CAR during mitosis (left panel) and cytoplasmic filaments in interphase cells (right panel). (B) GFP-Cdc8 (top panel and green in bottom panel) colocalisation with actin (middle panel and red in bottom panel) was confirmed in merged images (bottom panel) of DPM751 cells stained with Rhodamine-conjugated phalloidin. (C) Real-time imaging of GFP-Cdc8 in live DPM809 cells revealed the dynamic nature of actin filaments in vivo. (D) Autofluorescence of DPM837 reveals the budding yeast tropomyosin TPM1 localises to the CAR in fission yeast cells. Rhodamine-phalloidin staining (Red) shows that GFP-Tpm1 (green) colocalises with actin (E). (F) Time-lapse imaging of DPM837 reveals GFP-Tpm1 recruits to a functional CAR. (G) Imaging of live DPM841 cells indicates smooth muscle Tm concentrate to the cell equator but fails to localise to the CAR in the presence of wild type Cdc8; but localises to the CAR in cells bearing the *cdc8-110* allele (DPM924) when incubated at 36°C (H). (I) Overexpressed GFP–smooth-muscle-Tm concentrates to a single fluorescent amorphous cytoplasmic aggregate and brings about an accumulation of uninucleate elongated cells (GFP, green; phase, red). Bars, 2 μm.

recruiting to the CAR during mitosis (Fig. 3G). In contrast to Cdc8, when Tpm1, Tpm2 or either of the metazoan GFP-Tms were overexpressed, the fusion proteins concentrated to a single large bright aggregate within the cytoplasm (Fig. 3I), which was not associated with actin (not shown). An additional consequence of overexpressing Tm is that elongated uninucleate cells accumulated within the culture – a phenotype synonymous with a cell cycle arrest.

Next, the ability of Tpm1, Tpm2, smooth Tm and skeletal Tm to complement the temperature-sensitive *cdc8-110* allele was examined (Fig. 4A,B) in *cdc8-110* cells in which genes encoding each Tm had been integrated into the genome and were under the control of the nmt41 promoter. Cultures were incubated at 36°C for 4 hours and the number of nuclei in 200 cells was examined. Only cultures of cells expressing Cdc8 or smooth muscle Tm had the normal percentage of binucleate aseptate cells (12%), whereas cells expressing Tpm1, Tpm2 or skeletal Tm accumulated as bi-nucleate and tetra-nucleate cells, demonstrating an inability to complement Cdc8 function.

Growth curves were generated for each strain at 36°C (Fig. 4B). Only smooth muscle Tm was able to fully complement the temperature-sensitive *cdc8-110* allele (Fig. 4B, orange line), producing a growth curve indistinguishable from cells expressing Cdc8 (Fig. 4B, black line). Budding yeast TPM1 and TPM2 were only able to partially complement the *cdc8-110* mutation (Fig. 4B, blue and green lines, respectively); however, the cells grew significantly slower than strains expressing either *cdc8* or the smooth muscle Tm. Skeletal muscle tropomyosin (Fig. 4B, dark blue line), was the only Tm examined that failed to form any colonies on plates incubated at 36°C (data not shown). These data indicate that only Cdc8 and smooth muscle Tm were capable of fully complementing Cdc8 function when they were stably expressed at levels equivalent to the endogenous Cdc8 protein.

We were surprised that smooth muscle Tm was able to complement Cdc8 function, yet failed to localise to actin filaments. One possibility was that its failure to localise was a result of it being unable to compete with Cdc8 for actin binding. We therefore examined GFP–smooth-Tm localisation in a *cdc8-110* strain, and found that in this background it localised to actin filaments (Fig. 3H), which indicates that although smooth muscle Tm is able to complement Cdc8 function, it is unable to compete with the endogenous protein for actin binding in vivo.

Cdc8 is acetylated in vivo

To establish the significance of Cdc8 migration as a doublet on SDS-PAGE gels, Cdc8 was purified from fission yeast cells. Silver staining revealed the purified protein migrated on 12.5% SDS-PAGE gels as a doublet (Fig. 4C) – both bands were recognised by the Cdc8 antisera (Fig. 4D). As in cell extracts, ~80% of the purified Cdc8 migrated in the faster migrating band. The purity and mass of the protein was determined by electron-spray mass spectroscopy, and revealed two peaks of 18,964.7 Da and 19,005.5 Da (Fig. 4E) mass. The masses of the peaks are consistent for a mixed population of unacetylated and acetylated Cdc8 (predicted masses are 18,964 and 19,006 respectively), and the inability to sequence the purified endogenous protein indicates that this occurred at the N-terminus of the protein. The relative size of the peak of the larger polypeptide was approximately four times that of the

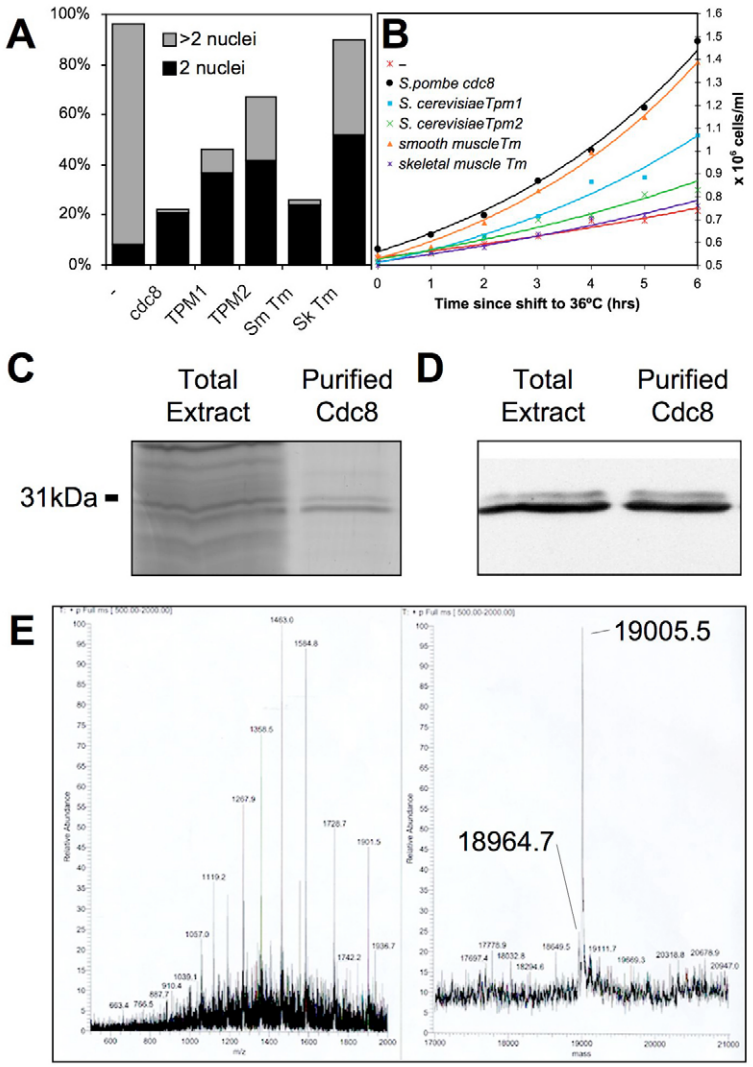

Fig. 4. Cdc8 is acetylated in vivo. (A,B) *cdc8-110* cells expressing additional integrant Tm genes under the control of the nmt41 promoter were grown at 36°C in EMM2 lacking thiamine. (A) The percentage of cells with two (black bars) or more than two (grey bars) nuclei were scored for each strain after 4 hours. (B) Growth curves generated for each strain over a 6 hour growth at 36°C. Only Cdc8 and smooth muscle Tm were capable of fully complementing the *cdc8-110* mutation. Endogenous Cdc8 was purified from mid-log phase *S. pombe* cells and analysed alongside total protein extracts by silver staining of SDS-PAGE gels (C) and western blot analysis using Cdc8 antisera (D). A single doublet migrating at ~30kDa was revealed by silver staining (C), while Cdc8 antisera recognised identical doublets in each lane. (E) Mass spectroscopy analysis of the purified endogenous Cdc8 revealed ~20% of this protein had a mass of 18964.1 (predicted mass of Cdc8: 18,964.7 Da), while the remaining 80% had a mass pf 19005.5 Da, which corresponds to the predicted mass of acetylated Cdc8.

smaller one, suggesting that the faster migrating Cdc8 band on SDS-PAGE gels is an acetylated form of the protein.

Affinity of endogenous and recombinant Cdc8 tropomyosin for actin

It has been suggested that acetylation stabilises Tm's coiled-coil structure at the amino terminus (Palm et al., 2003), allowing Tm dimers to interact to form filaments capable of associating with F-actin cables (Cammarato et al., 2004). We wished to explore whether acetylation could play a similar role in modifying the affinity of Cdc8 for actin and therefore the in vivo function in *S. pombe*.

When recombinant tropomyosins are expressed in *E. coli*, they fail to become acetylated on their N-terminal Met residue, allowing the opportunity to examine the actin-binding properties of unacetylated Cdc8. A modified Cdc8 isoform with an Ala-Ser di-peptide amino extension (Cdc8-AS) was also heterologously produced. This modification mimics acetylation in studies of other Tms (Greenfield et al., 1994; Maytum et al., 2000; Monteiro et al., 1994). Mass spectroscopic analysis of recombinant protein confirmed the isolation of unacetylated proteins of masses 18964.3 Da and 19122.4 Da respectively. The actin affinity of each recombinant protein was determined, and compared with that of the endogenous Cdc8 dimer purified from *S. pombe*.

An example of an SDS-PAGE gel used for determining binding affinities is illustrated in Fig. 5A. The two gels shown represent a co-sedimentation experiment involving recombinant Cdc8. The top gel shows the pellet fractions, and the bottom gel illustrates the supernatant fractions. All samples contain 10 μM actin incubated with increasing concentrations of Cdc8 dimer from left (lane 1) to right (lane 14). In both gels, actin is the top band, the density of which remains constant in all the samples. The lower, faster migrating band is Cdc8, the density of which increases from the lowest to the highest Cdc8 dimer concentrations. Data for the three Cdc8 dimer isoforms were plotted and resulted in binding curves of sigmoidal shape, consistent for a Tm-binding curve (Fig. 5B). The binding coefficients ($K_{50\%}$) were determined after fitting the cooperative binding curves using the Hill equation (Table 1).

Co-sedimentation assay gels of endogenous Cdc8 purified from *S. pombe* (Fig. 5C) revealed the faster migrating component of the doublet has a higher affinity for actin than the slower band. The majority of the slower migrating

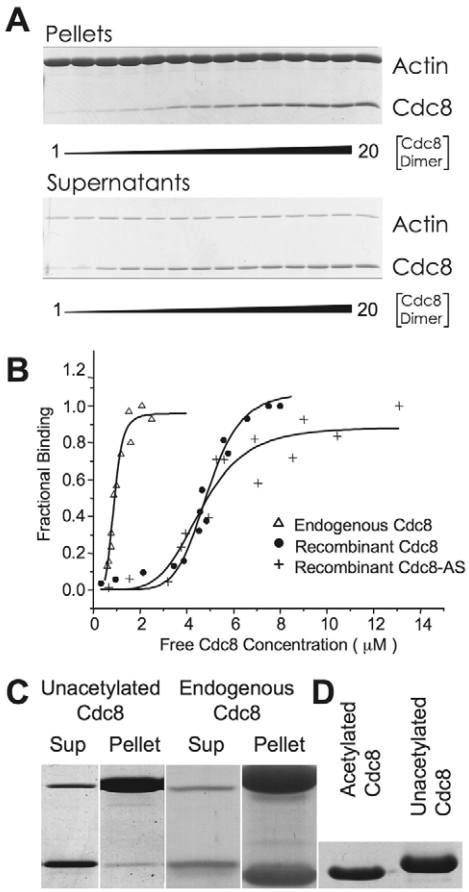

Fig. 5. Cdc8 requires N-terminal acetylation to associate with actin filaments. (A) 10 μM actin incubated with increasing concentrations of heterologous Cdc8 (1-20 μM in experiment shown) at 20°C for 30 minutes in 20 mM MOPS, 30 mM KCl, 5 mM $MgCl_2$, pH 7.0. The actin was pelleted at 100,000 ***g*** and the equivalent samples of the pellet (upper panel) and supernatant (lower panel) were run on an SDS-PAGE gel, which was stained with Coomassie Blue. (B) Binding constants ($K_{50\%}$) were measured as the free Tm dimer concentration at which the actin filament is half saturated by Cdc8 dimer, and was determined as the ratio of density of actin against the free concentrations of Cdc8 (circles), Cdc8-AS (+) or endogenous Cdc8 (△) dimers, as measured by quantitative analysis of supernatant and pellet co-sedimentation gels (A), and calculated using the Hill equation (see Table 1). (C) Supernatant and pellet co-sedimentation gels of unacetylated and endogenous Cdc8. The faster migrating endogenous Cdc8 band associated with actin in the pellet, while the slower migrating band was the prominent form in the supernatant. (D) Endogenous Cdc8 purified from actin co-sedimentation pellets from C migrated more slowly than unacetylated Cdc8 purified from *E. coli*.

endogenous Cdc8 remains in the supernatant in co-sedimentation assays. The two isoforms of endogenous Cdc8 were purified from the supernatant and pellet assay fractions (Fig. 5D), and mass spectroscopy revealed the faster migrating Cdc8 band is acetylated, whereas the slower form is unacetylated. Therefore we can conclude that 80% of the Cdc8 is constantly acetylated throughout the cell cycle (Fig. 1B).

In contrast to the budding yeast, skeletal, and smooth muscle tropomyosins, the presence of the AS insertion at the N-terminus of Cdc8 had little affect on its actin affinity. Unlike many tropomyosins, unacetylated Cdc8 binds cooperatively to actin. The acetylated endogenous Cdc8 has a ~tenfold tighter affinity for actin than either recombinant protein. Sequence analysis revealed there is a significant divergence in the N-terminal region adjacent to the predicted amino overlap region (McLachlan and Stewart, 1975) of Cdc8 when compared with other Tms (Fig. 6A), suggesting this region is important in regulating the filament formation.

Table 1. Actin-binding properties of yeast tropomyosins

Protein (Dimer)	Origin	K_{50} (μM)	Reference
Cdc8	*E. coli*	4.9	This study
Cdc8-AS	*E. coli*	5.5	This study
Cdc8	*S. pombe*	0.6	This study
Tpm1/Tpm2	*E. coli*	–	(Maytum et al., 2000)
Tpm1-AS	*E. coli*	0.3-0.8	(Maytum et al., 2000)
Tpm2-AS	*E. coli*	~0.5	(Maytum et al., 2001)

Cdc8 regulates myosin binding to actin

We wished to explore whether Cdc8 played a role in regulating the interaction of myosin with actin. Pyrene-labelled actin was titrated with myosin motor domains under equilibrium binding conditions to assess whether the different Cdc8 proteins could regulate the binding of myosin motor domains (now referred to as myosin) to actin. Each titration was repeated, and representative data is presented in Fig. 6B, which show plots of the raw data (grey lines) in which myosin had been titrated against phalloidin-stabilised pyrene actin or pyrene actin saturated with Cdc8, Cdc8-AS or endogenous acetylated Cdc8 dimers. The plot for actin alone is shown on each graph for comparison. The sigmoidal shapes of the curves obtained for all three isoforms indicate that Cdc8 has an innate ability to regulate myosin binding by causing an initial inhibition of myosin binding (compare to actin alone), however this inhibition is most dramatic in the presence of acetylated Cdc8. Curves were fitted to a two-state model (Maytum et al., 2000; McKillop and Geeves, 1993), to take into account the absence of control proteins such as troponin in this system. The best fits for each Cdc8 isoform (black lines) were superimposed onto the same axes as the corresponding raw data. Table 2 shows the K_1 (association constant for actin binding to myosin), K_T (the equilibrium between the on and off states of actin, also called the C and M states) and *n* (cooperative unit size), values that were calculated for each Cdc8 isoform. The affinity of myosin for actin (K_1) did not vary dramatically between the three Cdc8 proteins (Table 2). Owing to the low sigmoidity of the Cdc8 and Cdc8-AS curves, the cooperative unit size (*n*) cannot be clearly defined using this system. In conclusion, the ability to regulate myosin binding to actin is an intrinsic property of Cdc8, and this inhibitory affect is in turn enhanced upon Tm acetylation.

Cdc8 filaments regulate myosin by occupying the closed position on actin

Myosin binding is regulated by changes in the position the Tm strand sits upon the actin filament. Structural and biochemical studies have demonstrated that skeletal tropomyosin can bind to actin filaments in a blocked, closed or open position, which have decreasing inhibitory effects on myosin binding to actin

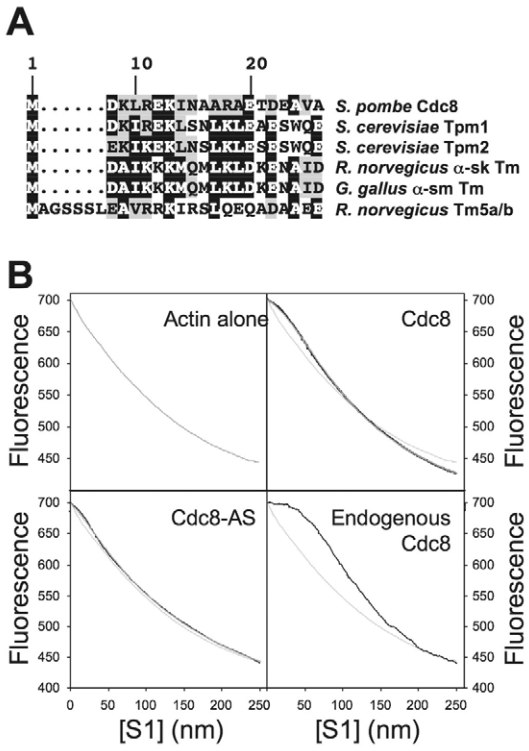

Fig. 6. Acetylated Cdc8 regulates myosin function in vitro. (A) Bioinformatic analysis reveals divergence within the N-terminus of *S. pombe* Cdc8. (B) Titration curves for myosin binding to either 50 nM phalloidin-stabilised pyrene-labelled actin alone (light grey line) or actin saturated with unacetylated Cdc8, Cdc8-AS or endogenous Cdc8 (black line). Curves of best fit data are superimposed on each Cdc8 graph (dark grey). The actin curve is present for reference in all graphs. Titration curves for each of the Cdc8 isoforms were sigmoidal in shape, demonstrating that all three have an inhibitory affect on myosin binding, although the inhibition is significantly stronger for the endogenous acetylated Cdc8.

(McKillop and Geeves, 1993; Vibert et al., 1997). One further way to elucidate the role of Cdc8 in myosin regulation is to examine whether acetylated Cdc8 affects the rate at which myosin binds to actin. Fast reaction kinetics experiments revealed that the presence of acetylated Cdc8 had no affect on the rate of initial myosin binding (not shown). This is consistent with Cdc8 filaments occupying the closed and not the blocked position on actin filaments, as the latter would inhibit binding and reduce the rate of myosin binding to actin. These data predict that Cdc8 filaments modulate myosin function by sitting predominantly in the closed position on actin filaments, thus inhibiting its initial binding until the tropomyosin moves cooperatively into the open position.

To confirm this, image reconstruction of electron micrographs of actin-Cdc8 filaments was carried out to reveal where Cdc8 strands sit on actin. In contrast to control F-actin samples lacking tropomyosin (Fig. 7A), yeast tropomyosin strands could be detected directly in electron micrographs of negatively stained F-actin–Cdc8 filaments (Fig. 7B) and was found coiling around the actin filaments with a characteristic pattern (Lehman et al., 1994) (Fig. 7B, arrows). In addition, excess unbound Cdc8 could be seen to form narrow elongated and continuous filaments, free of actin, in the background of F-actin and Cdc8 tropomyosin samples (not shown), suggesting that end-to-end bonded Cdc8 forms filaments are stable even in isolation (Flicker et al., 1982).

Helical reconstruction of single actin-Cdc8 filaments always showed tropomyosin strands in the closed position (n=15). Averages of eight filament reconstructions with the best phase agreement were constructed from micrographs of actin-Cdc8 filaments as described previously (Lehman et al., 1994; Lehman et al., 2000; Vibert et al., 1997). Surface views of F-actin-Cdc8 reconstructions revealed Cdc8 exclusively occupies the 'closed' position on actin (Fig. 8B,C), i.e. it localises on the outer edge of actin subdomains 3 and 4 next to the cleft separating the inner (subdomains 3 and 4) and outer (subdomains 1 and 2) domains of actin, which is the same position previously described for tropomyosin alone or troponin-tropomyosin-regulated filaments in the presence of Ca^{2+} (the closed or Ca^{2+}-induced position) (Lehman et al., 1994; Lehman et al., 2000; Pirani et al., 2005). Helical projections (Fig. 8D,E) and transverse sections (F and G) of maps of the 3D reconstructions confirmed the positional specificity of the tropomyosin strands in the closed position. Reconstructions of actin-Cdc8 filaments were displayed at 5 and 10 sigma above the mean density (Fig. 8B,C respectively), and corresponded to a resolution of 26 Å. The Cdc8 density is seen to form a continuous strand at a five times higher threshold than normally considered the industry standard. The density cross-section is consistent with Cdc8 existing as a dimer. The ability to observe continuous tropomyosin density at such high threshold levels in reconstructions (sigma=10) suggests a level of precision greater than that for the binding of other tropomyosins, such as for skeletal muscle α-tropomyosin in the absence of troponin, in comparable actin-tropomyosin complexes (Lehman et al., 2000; Pirani et al., 2005).

Discussion

The tropomyosins play a key role in regulating the dynamics of actin filaments in cells as diverse as muscle fibres and yeast. Their function requires that the protein forms parallel dimers that polymerise head to tail to generate strands which coil

Table 2. Parameters of fits for titration curves

Protein (Dimer)	K_1 ($\times 10^4\ M^{-1}$)	K_T	K_2	n	Reference
Cdc8	3.36	0.47	200	7	This study
Cdc8-AS	2.39	0.99	200	ND*	This study
Acetylated Cdc8	5.37	0.02	200	7	This study
Tpm1-AS	4.43	0.37	200	9	(Maytum et al., 2000)
Tpm2-AS	4.22	0.33	200	7	(Maytum et al., 2001)

*ND, not determined.

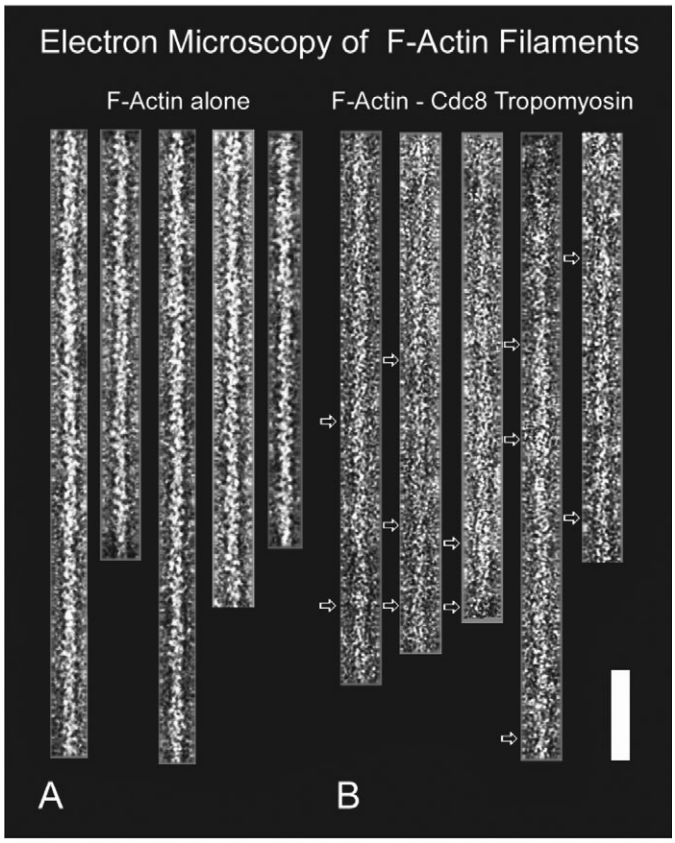

Fig. 7. Electron micrographs of F-actin-Cdc8 complexes. Negative staining of (A) F-actin alone (no tropomyosin), (B) F-actin-Cdc8; note the obliquely oriented strands that are characteristic of tropomyosin (Lehman et al., 1994) (several are indicated with arrows, and are best seen by viewing the figure at a glancing angle). When compared with control F-actin, the actin subunit structure of the decorated filaments appeared less well defined, owing to the binding of additional protein. Occasionally, unbound Cdc8 formed very narrow but elongated and continuous filaments, visible in samples of F-actin and Cdc8 tropomyosin (not shown). Bar, 50 nm.

around actin filaments providing stability to the polymer. The position the Tm strand sits upon the actin cable cannot only affect the stability of the thin filament, but also regulates the interaction of myosin with actin. The two budding yeast Tms both have crucial but non-overlapping roles in stabilising actin filaments, upon which myosin motors transport cargoes (Drees et al., 1995; Liu and Bretscher, 1992). By contrast, the fission yeast *S. pombe* possesses a single tropomyosin, which is essential for formation and contraction of the CAR (Balasubramanian et al., 1992). It is also required for the maintenance of polarised cell growth as demonstrated by the dumbbell-shaped morphology of cells lacking functional Cdc8 (Chang et al., 1996; Pelham, Jr and Chang, 2001). Here we report that in addition to stabilising actin filaments throughout the cell cycle, Cdc8 can also regulate myosin function.

In this study, we have carried out a detailed analysis of the biochemical, molecular and cell biological properties of Cdc8, which has facilitated the further elucidation of its cellular function. Parallel localisation studies using either an anti-Cdc8 antibody or a functional GFP-Cdc8 fusion protein confirmed Cdc8 localisation at the CAR. In addition, Cdc8 also localises with actin to a complex lattice of filaments, which extend throughout the cytoplasm of interphase cells. In addition, the novel *gfp-cdc8* strain described here has proven to be an invaluable tool to further investigate the dynamic nature of these filaments in vivo. The dynamic filaments were shown to coincide with actin, because their integrity was dependent upon polymerised actin. These findings are consistent with Cdc8 having a role both in maintaining CAR integrity during cell division and in stabilising actin filaments during interphase thus maintaining polarised cell growth (Balasubramanian et al., 1992; Ishiguro and Kobayashi, 1996; Pelham and Chang, 2001).

Using an anti-Cdc8 antibody in conjunction with mass spectroscopy it was possible to determine that Cdc8 protein levels did not vary and that 80% of the protein was N-terminally acetylated throughout the cell division cycle. Acetylation plays an important role in modulating the efficiency with which many tropomyosins interact with actin by modulating the structure of the N-terminus that facilitates head-to-tail interactions of Tm dimers (Hitchcock-DeGregori and Heald, 1987; Palm et al., 2003; Urbancikova and Hitchcock-DeGregori, 1994). This is certainly the case in budding yeast where recombinant Tpm1 and Tpm2 require the addition of an Ala-Ser (AS) dipeptide, which is a good mimic of N-terminal acetylation for metazoan Tms (Monteiro et al., 1994), to see any detectable association with actin (Maytum et al., 2000; Maytum et al., 2001).

Expression of GFP-Tm fusion proteins in fission yeast cells allowed the opportunity to compare the ability of each Tm to localise with its ability to function in *S. pombe*. Of the Tms examined, only Cdc8 and smooth muscle Tm were able to localise and function in vivo, however the smooth muscle Tm could not compete with the fission yeast Tm for actin binding in vivo. Budding yeast Tpm1 was able to localise but only partially complement Cdc8 function. However, Tpm2 failed to localise, which may be explained by the fact that Tpm2 lacks an internal region conserved in Tpm1 and Cdc8, which may be essential for Tm function in *S. pombe*. Biochemical analysis revealed that unmodified recombinant Cdc8 is capable of associating with actin, albeit with a low affinity, which is in contrast to either budding yeast Tm, and may in part explain why both Tpm1 and Tpm2 were unable to complement Cdc8 function in vivo. Tpm2 and skeletal Tm fusion proteins both concentrate near the CAR during mitosis, yet actin filament association was barely detectable. In addition, overexpression of Tpm1, Tpm2, smooth or skeletal muscle Tm resulted in an accumulation of elongated uninucleate cells. As it is only possible for two Tm filaments to simultaneously associate with the same single actin polymer, overexpressing Tm will not make more Tm associate with actin filaments. The arrest we observe is therefore probably brought about by either disrupting the dynamic properties of fission yeast actin filaments or by triggering a stress response. Consistent with the latter, actin is not seen to associate with the aggregate, and we observe no defects when we overexpress Cdc8 in *S. pombe* cells. However, the precise nature of the arrest is currently under investigation.

Purifying endogenous Cdc8 from fission yeast cells in milligram quantities allowed the opportunity to define the

actin-binding constant of an endogenous yeast Tm for the first time. This has revealed that N-terminal acetylation of Cdc8 results in its binding to actin with an affinity similar to that of both Tpm1-AS and Tpm2-AS from budding yeast, but a tenfold tighter affinity than for unmodified Cdc8. Similarly, in co-sedimentation assays of endogenous Cdc8, acetylated Cdc8 was exclusively seen in the actin pellet, whereas the supernatant predominantly contained the unacetylated isoform. It is unclear at this stage why a significant sub-population of the cellular Cdc8 is unmodified, but this is currently under investigation. However, analysis of Cdc8 from cells lacking F-actin suggests that Cdc8 acetylation is not dependent upon other components of the actin cytoskeleton (data not shown).

Surprisingly, addition of an Ala-Ser dipeptide at the N-terminus did not mimic Cdc8 N-terminal acetylation, because the $K_{50\%}$ for Cdc8-AS was not significantly different from unacetylated Cdc8. Why Cdc8 should behave so differently from other Tms is unclear; however, there is significant divergence in the N-terminal Cdc8 sequence adjacent to the predicted 8-10 amino acid head-to-tail overlap region for this Tm (McLachlan and Stewart, 1975), which could have a significant affect upon Tm-Tm contacts.

We have not yet determined whether any of the non-endogenous Tms are acetylated in fission yeast, but the fact that only smooth Tm can bind to actin in the absence of N-terminal modification whereas Tpm1, Tpm2 and skeletal Tm do not (Coulton et al., 2006; Maytum et al., 2001) may explain why only smooth muscle Tm was able to function in yeast (Fig. 4A,B). In addition, skeletal Tm requires the interaction of the troponin complex in order to bind actin with a high affinity, which may explain why this protein failed to either localise or function in *S. pombe*. Although endogenous *S. cerevisiae* Tpm1 has been purified and shown to associate with actin previously, neither the $K_{50\%}$ or K_T equilibrium constants have yet been defined for endogenous acetylated forms of either of the budding yeast Tms. Study of acetylated Tpm1 and Tpm2 may reveal whether the AS insertion mimics the true nature of acetylation for any of the fungal Tms.

The fact that Cdc8 binds to actin raises the possibility that it may also have a role in regulating myosin function. Cdc8 confers cooperativity (sigmoidal titration curves) on the myosin motor domain binding to actin, which indicates a potential to regulate myosin binding. The low value of K_T (the equilibrium constant between the closed and open forms of the filament) indicates that in the absence of myosin the Cdc8 spends 98% of its time in the C or 'off' state. This value of K_T is much smaller than for most tropomyosins studied to date (K_T=0.02) and suggests that the C-state is stabilised relative to the O-state (Lehman et al., 2000; Maytum et al., 1999; Pirani et al., 2005).

A number of recent studies suggest that movement of Tm on actin between these different conformations is related to the flexibility of the protein (Bacchiocchi et al., 2004; Chen and Lehrer, 2004; Heller et al., 2003; Lehrer et al., 1997; Singh and Hitchcock-DeGregori, 2003), with more rapid transitions being seen with flexible Tms. For Cdc8, removal of the acetylation group results in K_T being reduced from 0.02 to 0.47, i.e. the open state occupancy rises from 2% to 32%. Thus the increased stability of head-to-tail interactions facilitated by acetylation increases the stability of the Cdc8 strand in the closed conformation on actin. Polymerised acetylated Cdc8 may

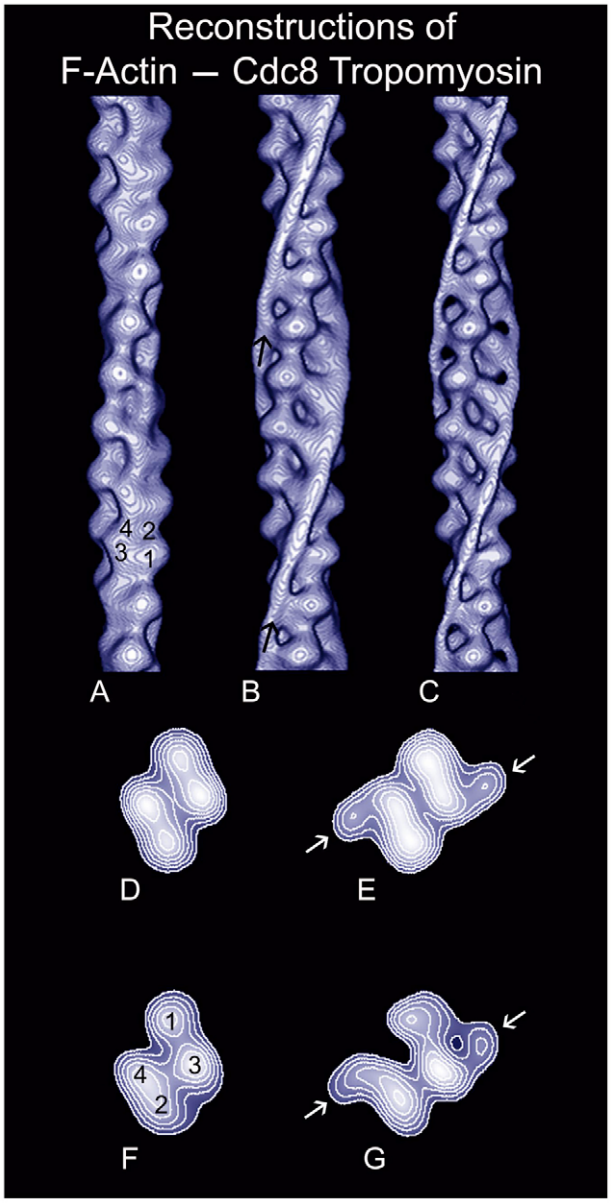

Fig. 8. Three-dimensional reconstructions of negatively stained thin filaments. Surface views of reconstructions of (A) F-actin control filaments (actin subdomains 1 to 4 marked on one actin monomer) and (B,C) F-actin-Cdc8. Additional density corresponding to tropomyosin (arrows) is observed for the filaments containing Cdc8. Cdc8 occupies the 'closed' position on actin, i.e. it localises on the outer edge of actin subdomains 3 and 4 next to the cleft separating the inner (subdomains 3 and 4) and outer (subdomains 1 and 2) domains of actin, which is the same position previously described for troponin-tropomyosin-regulated filaments in the absence of Ca^{2+} (Lehman et al., 1994; Vibert et al., 1997). Reconstructions were displayed at 5 sigma above the mean density in A and B and at 10 sigma in C; note the Cdc8 density forms a continuous strand even at very high threshold values. Helical projections (D,E) and transverse sections (F,G) of maps of the 3D reconstructions in A and B. (D,F) F-actin (E,G), F-actin-Cdc8. Actin subdomains numbered in (F). Helical projections (i.e. densities in the reconstructions projected onto a plane perpendicular to the axis of the filament), which show the average location of Cdc8 (arrows) on the inner domain of actin (E). Transverse sections show that the densities associated with Cdc8 are adjacent to subdomains 2 and 4 of actin (G). Also note that Cdc8 is not observed on pure actin filaments (no Cdc8) (A,D,F).

therefore have a reduced flexibility or higher affinity for actin in the C-state when compared with other Tms, with acetylation modulating the stability or interactions of the Cdc8 strand. These data are consistent with the finding that only Tms with a low K_T (i.e. smooth muscle Tm and fibroblast Tm) are capable of complementing Cdc8 function in vivo, providing strong evidence that unlike the budding yeast Tms, Cdc8 has essential roles in regulating myosin function in addition to stabilising actin filaments (Balasubramanian et al., 1992; Coulton et al., 2006; Maytum et al., 2001).

These data are consistent with the high quality of the EM reconstructions for the actin-Cdc8 filaments. These filaments show less variability than other actin-Tm filaments studied to date. This is consistent with the Cdc8 being predominantly in a single (i.e. closed) conformation. Unfortunately, because of its low actin affinity, it is not experimentally feasible to examine the position of unacetylated Cdc8 upon actin filaments by electron microscopy at this time.

EM studies of actin-Cdc8 filaments suggest that Cdc8 does not require actin to form a number of stable end-to-end interactions. Preliminary EM studies of rotary-shadowed Cdc8 reveals strands in the absence of actin – a property not reported for other tropomyosins – again showing increased strength of Tm-Tm contacts. Yeast mutant analysis may provide a means by which to explore the structure and stability of Tm filaments. It is intriguing to speculate that the rigid conformation of the acetylated Cdc8 may affect the actin polymer, thus increasing the energy requirement to move Cdc8 into the open position. Overlay comparison of the structure of actin filaments in the absence and presence of acetylated Cdc8 suggests a reproducible and consistent difference in the position of the actin densities (not shown). However the small sample size in this study does not provide conclusive evidence for this hypothesis at present.

The cellular requirement for actin filaments with tropomyosin strand formation remains unclear. We show here that Cdc8 can form stable complexes with actin and can have the potential to regulate the interaction of myosin motors with actin. How such a regulation would work in the cell remains undefined, and is currently being explored within our laboratory. However, a previous study provides in vivo evidence for a role of Tm in regulating unconventional myosin function in non-muscle cells (Tang and Ostap, 2001). Using a genetically tractable system, such as yeast, will allow the opportunity to rapidly define regulator proteins and regions within the Tm dimer required for it to regulate myosin-actin association in non-muscle cells.

Materials and Methods

Yeast cell culture and strains

The strains used in this study are listed in supplementary material Table S1. Cell culture and maintenance were carried out as described (Moreno et al., 1991). Cells were grown in minimal medium (EMM2) supplemented with the appropriate amino acids. Synchronous cultures were generated by transient arrest using the *cdc25-22* mutation in a strain possessing the *myo2-gfp* allele (Mulvihill and Hyams, 2002).

Molecular biology

S. pombe cdc8$^+$ cDNA was isolated from fission yeast genomic DNA using Expand High fidelity polymerase with the primers oDM111 (5′-CATATGGATAAGCTT-AGAGAGAAAATTAATGCCGCTCGT-3′) and oDM112 (5′-GGGCCCCTACAA-ATCCTCAAGAGCTT-3′), cloned into pTOPO2.1 (Invitrogen) and sequenced (creating pTOPO*cdc8*$^+$). The *cdc8-AS* allele was created by PCR using primers oDM109 (5′-CATATGGCTAGCATGG-ATAAGCTTAGAGAGAAAAT-3′) and oDM112, cloned into pTOPO2.1 and sequenced (creating pTOPO*cdc8-AS*). The *cdc8*$^+$ and *cdc8-AS* alleles were subsequently cloned into the pJC20 bacterial T7 expression vector (Konrad, 1993), and the *S. pombe* expression plasmids pREP41, pINT41 and pINT41NGFP (Craven et al., 1998). cDNA encoding for smTM, skTM, TPM1 and TPM2 were isolated from lab stocks, sequenced and each cloned into the *Nde*I-*Bam*HI sites of pINT41 and pINT41NGFP.

Immunological techniques

Standard immunological methods were used as described (Harlow and Lane, 1988). Anti-Cdc8 antibodies were created by immunising an SPF rabbit with purified full-length recombinant Cdc8 protein with Titre Max Gold adjuvant. Sera were collected at 1-month intervals 1 week after each boost.

Western blotting

5×10^7 cells were harvested from mid-log phase cultures of *S. pombe* cells, washed in ice-cold STOP buffer (Simanis and Nurse, 1986), and frozen in liquid nitrogen prior to storage at –80°C. Protein was extracted by resuspending cells in EXPY buffer [HE buffer (Simanis and Nurse, 1986) supplemented with 1 μg/ml AEBSF, 1 μg/ml antipain, 1 μg/ml aprotinin, 10 μM benzamidine, 1 μg/ml chymostatin, 1 μg/ml E64, 1 μg/ml leupeptin, 1 μg/ml pepstatin, 5 μM phenanthroline, and 1 mM PMSF] and disrupting them with 500 μl of acid-washed glass beads in a ThermoSavant Fastprep 120 (MP Biochemicals, Irvine, CA). Samples were then boiled with SDS-PAGE loading buffer. Western blotting detection was carried out using alkaline phosphatase reagents. Cdc8 levels were determined by measuring band intensities on the scanned blot using Scion image software. Cdc8 serum was used at a concentration of 1:1000, anti-GFP antibodies (generous gift from W. Gullick, University of Kent, UK) were used at 1:100 and TAT1 anti-α-tubulin antibodies were used at 1:100 (Woods et al., 1989).

Fluorescence microscopy

Immunofluorescence microscopy was performed as described (Hagan and Hyams, 1988) except glutaraldehyde was omitted. Anti-Cdc8 sera was used at a dilution of 1:100. Cells were visualised using an Olympus IX71 microscope with PLAPO100XO/TIRFM-SP/1.45NA lens mounted on a PIFOC® Z-axis focus drive (Physik Instruments, Karlsruhe, Germany) and illuminated with an automated 300W Xenon light source (Sutter, Novato, CA) with appropriate filters. Micrographs were captured with a Coolsnap HQ digital camera (Roper Scientific, Tucson, AZ) controlled with Metamorph software (Molecular Devices, Downington, PA). Live cells were grown, visualised, captured and images were processed as described previously (Grallert et al., 2004).

Protein purification

Recombinant Cdc8, and Cdc8-AS proteins were expressed (from pJC20*cdc8*$^+$ and pJC20*cdc8-AS*) in BL21 DE3 cells. Mid-log cultures were grown for 3 hours with 100 mg/l IPTG. Cells were harvested, resuspended in 30 ml lysis buffer (20 mM Tris-HCl pH 7.5, 100 mM NaCl, 2 mM EGTA and 5 mM $MgCl_2$), lysed by sonication and heated at 80°C for 10 minutes. Denatured proteins were removed by centrifugation. The soluble Cdc8 was isolated by isoelectric precipitation at pH 4.55, resuspended in 20 ml FPLC running buffer (5 mM PO_4^- pH 7.0, 100 mM NaCl) with 10 mg/l DNase and 10 mg/l RNase, and incubated at 4°C for 2 hours. The Cdc8 was purified twice by FPLC using 2 × 5 ml Pharmacia HiTrap-Q columns in tandem, by elution with a 100-900 mM NaCl gradient. Cdc8 was isolated from appropriate fractions by isolectric precipitation at pH 4.55 and resuspended in 5 mM Tris-HCl pH 7.0. The purity and mass of the proteins were determined by mass spectroscopy, while parallel Bradford, gel densitometry and spectroscopic analyses determined protein concentrations. Endogenous Cdc8 was isolated from cells from 20 litres of mid-log fission yeast cells. Harvested cells were resuspended in EXPY buffer, cell walls were disrupted, and incubated at 80°C for 10 minutes. Endogenous Cdc8 was purified by isoelectric precipitation and FPLC as for recombinant Cdc8. Rabbit actin was purified as described previously (Spudich and Watt, 1971).

Co-sedimentation assays and fluorescence titrations

These were undertaken as described previously (Coulton et al., 2006) using a modified version of the McKillop and Geeves model (Maytum et al., 1999).

Electron microscopy and helical reconstructions

Cdc8 purified from *S. pombe* (endogenous) (120 μM) was mixed with F-actin (24 μM), to allow Cdc8-actin filament formation, in buffer containing 20 mM MOPS, pH 7.0, 30 mM KCl and 5 mM $MgCl_2$. The actin-Cdc8 filaments were diluted 20-fold in the same buffer immediately prior to applying to carbon-coated electron microscopy grids. Samples were negatively stained, electron microscopy images captured at 45,000× under low-dose conditions (~12e$^-$/Å), and helical reconstructions were carried out as described previously (Lehman et al., 2000; Moody et al., 1990; Owen et al., 1996).

We gratefully acknowledge Roger Craig (University of Massachusetts School of Medicine) for use of Electron Microscopy facilities, supported by NIH Shared Instrument grant RR08426 (to Roger Craig). We thank Agnes Grallert and Steve Bagley from the Patterson Cancer Research Institute for their time, advice and use of microscopes to capture Cdc8 filaments time-lapse sequences and

Victoria Hatch for technical assistance. We also thank members of the Geeves and Mulvihill labs for helpful discussions and comments on the manuscript. This study was funded by a BBSRC David Phillips Fellowship to D.P.M. and NIH grants HL36153 (to W.L.) and AR041637 (to M.A.G.).

References

Bacchiocchi, C., Graceffa, P. and Lehrer, S. S. (2004). Myosin-induced movement of alphaalpha, alphabeta, and betabeta smooth muscle tropomyosin on actin observed by multisite FRET. *Biophys. J.* **86**, 2295-2307.

Balasubramanian, M. K., Helfman, D. M. and Hemmingsen, S. M. (1992). A new tropomyosin essential for cytokinesis in the fission yeast S. pombe. *Nature* **360**, 84-87.

Balasubramanian, M. K., Hirani, B. R., Burke, J. D. and Gould, K. L. (1994). The Schizosaccharomyces pombe cdc3+ gene encodes a profilin essential for cytokinesis. *J. Cell Biol.* **125**, 1289-1301.

Bezanilla, M., Wilson, J. M. and Pollard, T. D. (2000). Fission yeast myosin-II isoforms assemble into contractile rings at distinct times during mitosis. *Curr. Biol.* **10**, 397-400.

Brown, J. H., Kim, K. H., Jun, G., Greenfield, N. J., Dominguez, R., Volkmann, N., Hitchcock-DeGregori, S. E. and Cohen, C. (2001). Deciphering the design of the tropomyosin molecule. *Proc. Natl. Acad. Sci. USA* **98**, 8496-8501.

Cammarato, A., Hatch, V., Saide, J., Craig, R., Sparrow, J. C., Tobacman, L. S. and Lehman, W. (2004). Drosophila muscle regulation characterized by electron microscopy and three-dimensional reconstruction of thin filament mutants. *Biophys. J.* **86**, 1618-1624.

Chang, F., Woollard, A. and Nurse, P. (1996). Isolation and characterization of fission yeast mutants defective in the assembly and placement of the contractile actin ring. *J. Cell Sci.* **109**, 131-142.

Chen, Y. and Lehrer, S. S. (2004). Distances between tropomyosin sites across the muscle thin filament using luminescence resonance energy transfer: evidence for tropomyosin flexibility. *Biochemistry* **43**, 11491-11499.

Coulton, A., Lehrer, S. S. and Geeves, M. A. (2006). Functional homodimers and heterodimers of recombinant smooth muscle tropomyosin. *Biochemistry* **45**, 12853-12858.

Craven, R. A., Griffiths, D. J., Sheldrick, K. S., Randall, R. E., Hagan, I. M. and Carr, A. M. (1998). Vectors for the expression of tagged proteins in Schizosaccharomyces pombe. *Gene* **221**, 59-68.

Drees, B., Brown, C., Barrell, B. G. and Bretscher, A. (1995). Tropomyosin is essential in yeast, yet the TPM1 and TPM2 products perform distinct functions. *J. Cell Biol.* **128**, 383-392.

Flicker, P. F., Phillips, G. N., Jr and Cohen, C. (1982). Troponin and its interactions with tropomyosin. An electron microscope study. *J. Mol. Biol.* **162**, 495-501.

Grallert, A., Krapp, A., Bagley, S., Simanis, V. and Hagan, I. M. (2004). Recruitment of NIMA kinase shows that maturation of the S. pombe spindle-pole body occurs over consecutive cell cycles and reveals a role for NIMA in modulating SIN activity. *Genes Dev.* **18**, 1007-1021.

Greenfield, N. J., Stafford, W. F. and Hitchcock-DeGregori, S. E. (1994). The effect of N-terminal acetylation on the structure of an N-terminal tropomyosin peptide and alpha alpha-tropomyosin. *Protein Sci.* **3**, 402-410.

Gunning, P. W., Schevzov, G., Kee, A. J. and Hardeman, E. C. (2005). Tropomyosin isoforms: divining rods for actin cytoskeleton function. *Trends Cell Biol.* **15**, 333-341.

Hagan, I. M. and Hyams, J. S. (1988). The use of cell division cycle mutants to investigate the control of microtubule distribution in the fission yeast Schizosaccharomyces pombe. *J. Cell Sci.* **89**, 343-357.

Harlow, E. and Lane, D. (1988). *Antibodies: A Laboratory Manual*. Cold Spring Harbor: Cold Spring Harbor Laboratory Press.

Heller, M. J., Nili, M., Homsher, E. and Tobacman, L. S. (2003). Cardiomyopathic tropomyosin mutations that increase thin filament Ca2+ sensitivity and tropomyosin N-domain flexibility. *J. Biol. Chem.* **278**, 41742-41748.

Hitchcock-DeGregori, S. E. and Heald, R. W. (1987). Altered actin and troponin binding of amino-terminal variants of chicken striated muscle alpha-tropomyosin expressed in Escherichia coli. *J. Biol. Chem.* **262**, 9730-9735.

Ishiguro, J. and Kobayashi, W. (1996). An actin point-mutation neighboring the 'hydrophobic plug' causes defects in the maintenance of cell polarity and septum organization in the fission yeast Schizosaccharomyces pombe. *FEBS Lett.* **392**, 237-241.

Kitayama, C., Sugimoto, A. and Yamamoto, M. (1997). Type II myosin heavy chain encoded by the myo2 gene composes the contractile ring during cytokinesis in Schizosaccharomyces pombe. *J. Cell Biol.* **137**, 1309-1319.

Konrad, M. (1993). Molecular analysis of the essential gene for adenylate kinase from the fission yeast Schizosaccharomyces pombe. *J. Biol. Chem.* **268**, 11326-11334.

Kurahashi, H., Imai, Y. and Yamamoto, M. (2002). Tropomyosin is required for the cell fusion process during conjugation in fission yeast. *Genes Cells* **7**, 375-384.

Lehman, W., Craig, R. and Vibert, P. (1994). Ca(2+)-induced tropomyosin movement in Limulus thin filaments revealed by three-dimensional reconstruction. *Nature* **368**, 65-67.

Lehman, W., Hatch, V., Korman, V., Rosol, M., Thomas, L., Maytum, R., Geeves, M. A., Van Eyk, J. E., Tobacman, L. S. and Craig, R. (2000). Tropomyosin and actin isoforms modulate the localization of tropomyosin strands on actin filaments. *J. Mol. Biol.* **302**, 593-606.

Lehrer, S. S., Golitsina, N. L. and Geeves, M. A. (1997). Actin-tropomyosin activation of myosin subfragment 1 ATPase and thin filament cooperativity. The role of tropomyosin flexibility and end-to-end interactions. *Biochemistry* **36**, 13449-13454.

Liu, H. P. and Bretscher, A. (1989). Disruption of the single tropomyosin gene in yeast results in the disappearance of actin cables from the cytoskeleton. *Cell* **57**, 233-242.

Liu, H. and Bretscher, A. (1992). Characterization of TPM1 disrupted yeast cells indicates an involvement of tropomyosin in directed vesicular transport. *J. Cell Biol.* **118**, 285-299.

Maytum, R., Lehrer, S. S. and Geeves, M. A. (1999). Cooperativity and switching within the three-state model of muscle regulation. *Biochemistry* **38**, 1102-1110.

Maytum, R., Geeves, M. A. and Konrad, M. (2000). Actomyosin regulatory properties of yeast tropomyosin are dependent upon N-terminal modification. *Biochemistry* **39**, 11913-11920.

Maytum, R., Konrad, M., Lehrer, S. S. and Geeves, M. A. (2001). Regulatory properties of tropomyosin effects of length, isoform, and N-terminal sequence. *Biochemistry* **40**, 7334-7341.

McKillop, D. F. and Geeves, M. A. (1993). Regulation of the interaction between actin and myosin subfragment 1, evidence for three states of the thin filament. *Biophys. J.* **65**, 693-701.

McLachlan, A. D. and Stewart, M. (1975). Tropomyosin coiled-coil interactions: evidence for an unstaggered structure. *J. Mol. Biol.* **98**, 293-304.

Monteiro, P. B., Lataro, R. C., Ferro, J. A. and Reinach, F. de C. (1994). Functional alpha-tropomyosin produced in Escherichia coli. A dipeptide extension can substitute the amino-terminal acetyl group. *J. Biol. Chem.* **269**, 10461-10466.

Moody, C., Lehman, W. and Craig, R. (1990). Caldesmon and the structure of smooth muscle thin filaments: electron microscopy of isolated thin filaments. *J. Muscle Res. Cell Motil.* **11**, 176-185.

Moreno, S., Klar, A. and Nurse, P. (1991). Molecular genetic analysis of fission yeast Schizosaccharomyces pombe. *Meth. Enzymol.* **194**, 795-823.

Mulvihill, D. P. and Hyams, J. S. (2002). Cytokinetic actomyosin ring formation and septation in fission yeast are dependent on the full recruitment of the polo-like kinase Plo1 to the spindle pole body and a functional spindle assembly checkpoint. *J. Cell Sci.* **115**, 3575-3586.

Nurse, P., Thuriaux, P. and Nasmyth, K. (1976). Genetic control of the cell division cycle in the fission yeast Schizosaccharomyces pombe. *Mol. Gen. Genet.* **146**, 167-178.

Owen, C. H., Morgan, D. G. and DeRosier, D. J. (1996). Image analysis of helical objects: the Brandeis Helical Package. *J. Struct. Biol.* **116**, 167-175.

Palm, T., Greenfield, N. J. and Hitchcock-DeGregori, S. E. (2003). Tropomyosin ends determine the stability and functionality of overlap and troponin T complexes. *Biophys. J.* **84**, 3181-3189.

Pelham, R. J., Jr and Chang, F. (2001). Role of actin polymerization and actin cables in actin-patch movement in Schizosaccharomyces pombe. *Nat. Cell Biol.* **3**, 235-244.

Perry, S. V. (2001). Vertebrate tropomyosin: distribution, properties and function. *J. Muscle Res. Cell Motil.* **22**, 5-49.

Pirani, A., Xu, C., Hatch, V., Craig, R., Tobacman, L. S. and Lehman, W. (2005). Single particle analysis of relaxed and activated muscle thin filaments. *J. Mol. Biol.* **346**, 761-772.

Pittenger, M. F. and Helfman, D. M. (1992). In vitro and in vivo characterization of four fibroblast tropomyosins produced in bacteria: TM-2, TM-3, TM-5a, and TM-5b are co-localized in interphase fibroblasts. *J. Cell Biol.* **118**, 841-858.

Polevoda, B., Cardillo, T. S., Doyle, T. C., Bedi, G. S. and Sherman, F. (2003). Nat3p and Mdm20p are required for function of yeast NatB Nalpha-terminal acetyltransferase and of actin and tropomyosin. *J. Biol. Chem.* **278**, 30686-30697.

Schott, D., Ho, J., Pruyne, D. and Bretscher, A. (1999). The COOH-terminal domain of Myo2p, a yeast myosin V, has a direct role in secretory vesicle targeting. *J. Cell Biol.* **147**, 791-808.

Simanis, V. and Nurse, P. (1986). The cell cycle control gene cdc2+ of fission yeast encodes a protein kinase potentially regulated by phosphorylation. *Cell* **45**, 261-268.

Singer, J. M. and Shaw, J. M. (2003). Mdm20 protein functions with Nat3 protein to acetylate Tpm1 protein and regulate tropomyosin-actin interactions in budding yeast. *Proc. Natl. Acad. Sci. USA* **100**, 7644-7649.

Singer, J. M., Hermann, G. J. and Shaw, J. M. (2000). Suppressors of mdm20 in yeast identify new alleles of ACT1 and TPM1 predicted to enhance actin-tropomyosin interactions. *Genetics* **156**, 523-534.

Singh, A. and Hitchcock-DeGregori, S. E. (2003). Local destabilization of the tropomyosin coiled coil gives the molecular flexibility required for actin binding. *Biochemistry* **42**, 14114-14121.

Spudich, J. A. and Watt, S. (1971). The regulation of rabbit skeletal muscle contraction. I. Biochemical studies of the interaction of the tropomyosin-troponin complex with actin and the proteolytic fragments of myosin. *J. Biol. Chem.* **246**, 4866-4871.

Tang, N. and Ostap, E. M. (2001). Motor domain-dependent localization of myo1b (myr-1). *Curr. Biol.* **11**, 1131-1135.

Umesono, K., Toda, T., Hayashi, S. and Yanagida, M. (1983). Cell division cycle genes nda2 and nda3 of the fission yeast Schizosaccharomyces pombe control microtubular organization and sensitivity to anti-mitotic benzimidazole compounds. *J. Mol. Biol.* **168**, 271-284.

Urbancikova, M. and Hitchcock-DeGregori, S. E. (1994). Requirement of amino-terminal modification for striated muscle alpha-tropomyosin function. *J. Biol. Chem.* **269**, 24310-24315.

Vibert, P., Craig, R. and Lehman, W. (1997). Steric-model for activation of muscle thin filaments. *J. Mol. Biol.* **266**, 8-14.

Woods, A., Sherwin, T., Sasse, R., Macrae, T. H., Baines, A. J. and Gull, K. (1989) Definition of individual components within the cytoskeleton of *Trypanosoma brucei* by a library of monoclonal-antibodies. *J. Cell Sci.*, **93**, 491-500.